

REMOTE SENSING-BASED BIOMASS MAPS FOR AN EFFICIENT USE OF FERTILIZERS

J.G.P.W. Clevers

*Centre for Geo-Information
Wageningen University
Wageningen, The Netherlands*

K.H. Wijnholds

*Applied Plant Research (PPO)
Valthermond, The Netherlands*

J.N. Jukema

*Applied Plant Research (PPO)
Lelystad, The Netherlands*

ABSTRACT

For decades the main objective of farmers was to get the highest yields from their farmland. Nowadays, quality of agricultural products is becoming more and more important for the largest returns. In addition, the effects on our environment are also becoming important. These put increasing limitations on modern agriculture. So-called site-specific management can optimize the input of, for instance, nutrients and pesticides to the need of the plants. In this study, the objective was to study whether spectral measurements are suitable for determining optimal nitrogen (N) fertilization levels in potatoes. For determining this optimal N level, two field trials were designed in a potato field. Both trials had four N levels in four replicates. Spectral measurements were performed with a Cropscan™ 8-band radiometer during the growing season. In addition to the spectral reflectances, the weighted difference vegetation index (WDVI) and the red-edge position (REP) were derived. Results show that WDVI and REP were significantly correlated with tuber yield and can be used for setting optimal N levels. Biomass maps can be created using remote sensing images for mapping relative differences within fields. Based on these maps the farmer can take site specific actions to improve his overall management within a parcel.

Keywords: Remote sensing, Precision farming, Biomass map, Spectroscopy, Red-edge index

INTRODUCTION

Monitoring agricultural crops during the growing season is important for observing growth and development of the crop. This can provide significant information in order to be able to adjust the growth of the crops, e.g. for applications in the field of precision farming. So-called site-specific management can optimize the input of, for instance, nutrients and pesticides to the need of the plants. In this way it can minimize negative effects on the environment, provide an optimal yield and/or provide an optimal product quality. Secondly, it can provide information to obtain yield predictions well before harvest time, which is of importance for decision making at various levels, for logistics and for trade activities. More and more use is being made of crop growth models for such monitoring activities. A serious drawback of crop growth models is the absence of an accurate spatial component. If a spatial component is included, the spatial information generally is only available at an aggregated level. Examples are meteorological and soil-related information. Remote sensing data provide information on the crop growth as a result of spatially heterogeneous soil and management factors. As a result, remote sensing data can be used for calibrating crop growth models for actual field conditions, thus rendering the combination of growth models and remote sensing data a valuable tool for growth monitoring (Clevers et al., 1994; Delecolle et al., 1992; Maas, 1988).

The spectral signature of leaves is dominated by chlorophyll in the visible (VIS) region of the electromagnetic spectrum, by the cell structure in the near-infrared (NIR) regions and by water content in the short-wave infrared (SWIR) regions. In addition to these variables, at the canopy level the leaf area index (LAI), the amount of green biomass and the leaf angle distribution determine the spectral signature. From a remote sensing point of view, the illumination and observation geometry are also important. Many studies have focused on the use of vegetation indices, calculated as combinations of NIR and red reflectance, for estimating and monitoring vegetation characteristics. These indices correlate well with plant variables such as biomass, LAI and the fraction of absorbed photosynthetically active radiation (Baret and Guyot, 1991; Broge and Leblanc, 2001; Daughtry et al., 2000).

A second type of indices focuses on the so-called red-edge region. Clevers (1999) showed that imaging spectrometry might provide additional information at the red-edge region, not covered by the information derived from a combination of a NIR and a VIS broad spectral band. It can be concluded that, concerning high spectral resolution data, this seems to be the major contribution of imaging spectrometry to vegetation studies. The remote sensing of foliar chemical concentrations, other than chlorophyll and water, has not been very successful due to among other things the presence of water in living leaf tissue.

Indices based on remote sensing information appear to be very suitable for mapping and monitoring growth differences of agricultural crops, but they do not provide a direct indication of the causes of these growth differences. This information has to be obtained in a different way. Since nitrogen is one of the most important fertilizers for agricultural crops, growth differences are often corrected by tuning nitrogen fertilization. Growth differences can also be caused

by other elements like potassium or phosphorous. The acidity of the soil or the occurrence of diseases can also be a factor. In this study we focus on determining the optimal nitrogen (N) fertilization level in potatoes. Main objective is to study whether spectral measurements are suitable for determining this optimal N level and subsequently which index can best be used.

SPECTRAL INDICES

As stated before, estimation of LAI of agricultural crops during the growing season can be based on using vegetation indices. Clevers (Clevers, 1988; Clevers, 1989) derived a simplified, semi-empirical reflectance model for estimating LAI (CLAIR model). In this model, first, the WDVI (weighted difference vegetation index) is ascertained as a weighted difference between measured near-infrared (NIR) and red reflectances, assuming that the ratio of NIR and red reflectances of bare soil is constant. In this way a correction for the influence of soil background is performed:

$$WDVI = NIR - (C \times R) \quad (1)$$

NIR = measured NIR reflectance;

R = measured red reflectance;

C = slope of the (soil-specific) soil line, or ratio between NIR and red reflectance of soil.

Subsequently, this WDVI is used for estimating LAI according to the inverse of an exponential function:

$$LAI = -1/\alpha \times \ln(1 - WDVI / WDVI_{\infty}) \quad (2)$$

with α and $WDVI_{\infty}$ as two empirical parameters.

The CLAIR model was evaluated for various crops (Bouman et al., 1992; Clevers, 1991). Ground-based reflectance measurements obtained in The Netherlands over different experimental fields during more than 10 years were used. For instance, a single regression line was found that was not significantly different for cereals like wheat, barley and oats during the vegetative growth period (before heading). Such ground-based parameter estimates could be applied to airborne (Clevers and Van Leeuwen, 1996) and satellite measurements (Clevers et al., 2002).

Horler et al. (1983) were among the first researchers to point out the importance of the red-NIR wavelength transition for vegetation studies. At red wavelengths, reflectance is low due to absorbance by chlorophyll pigments while in NIR wavelengths, reflectance is high due to scattering inside the leaf and multiple reflections inside the canopy, resulting in a steep rise in reflectance between 670 and 780 nm. Both the position and the slope of this red-edge change under stress conditions, resulting in a shift of the slope towards shorter wavelengths (Horler et al., 1983; Wessman, 1994). The red-edge position (REP)

is defined as the position of the inflection point of the red-NIR slope. This REP shift due to stress conditions can be caused both by a decrease in leaf chlorophyll concentration and by a decrease in LAI (Clevers and Jongschaap, 2001). These are the main variables determining the REP. The REP can be studied by plotting $dR/d\lambda$, the first derivative of reflectance (R) with respect to wavelength (λ), as a function of λ . Alternatively, in many studies simple functions have been fitted to the reflectance spectrum in the red-edge region, and subsequently the wavelength belonging to the maximum slope has been extracted from such an analytical expression.

Although an increasing number of airborne and spaceborne imaging spectrometers have become available, their spectral resolution is not fine enough for an accurate determination of the REP using derivative spectra. Therefore, fitting a mathematical function to a few measurements in the red-edge region is often applied to estimate the REP.

Guyot and Baret (1988) applied a simple linear model to the red-infrared slope. This method assumes that the reflectance curve at the red-edge can be simplified to a straight line between 700 and 740 nm. The reflectance of the REP is then estimated as being halfway the reflectance in the NIR at about 780 nm and the reflectance minimum of the chlorophyll absorption feature at about 670 nm. Subsequently, the REP is estimated by linearly interpolating between measurements at 700 and 740 nm, following:

$$REP = 700 + 40 \times \left(\frac{(R_{670} + R_{780})/2 - R_{700}}{R_{740} - R_{700}} \right) \quad (3)$$

where R_{670} , R_{700} , R_{740} and R_{780} are the reflectance values at 670, 700, 740 and 780 nm wavelength, respectively, and the constants 700 and 40 result from interpolation in the 700–740 nm interval.

METHODOLOGY

Set-up field experiment potatoes

In this study a potato field of 5 ha was used at the experimental farm “t Kompas” in Valthermond (the Netherlands). This experimental farm is part of the Institute for Applied Plant Research of Wageningen University and Research Centre. The fields are part of the project “Perceel Centraal”. The potatoes were planted on 19 April 2007 and harvested on 2 and 10 October 2007. The cultivar was Seresta. The farm is situated on a partly peaty and partly sandy soil type. Within the field two identical field trials were set up. One trial was put in a less humous and dryer part of the field (trial 1) and one trial was put in a more humous part (trial 2). Four nitrogen levels were applied in each trial (table 1).

Table 1. Levels of nitrogen fertilization applied in both trials.

N level	N application (kg/ha)
N0	0
N1	140
N2	200
N3	260

Table 2. Specifications of the Cropscan system.

Spectral position (nm)	band	Band width (nm)
490		6
550		7
670		9
700		10
740		11
780		12
870		13
1090		11

The lowest level (N0) did not receive any N fertilizers. N2 (200 kg/ha) matches the recommended fertilizer application based on soil type and N reserves in the soil at the beginning of the season. N1 and N2 are representing a deviation of 60 kg/ha below and above the recommended level, respectively. Within each trial four replicates were created, resulting in 16 plots per trial. Size of each net plot was 1.5×12 m. The field outside the trial areas received the recommended fertilization level too.

Cropscan

The Cropscan™ (Skye Limited Inc.) used in this study is a 8-band radiometer. It measures simultaneously the reflected and incoming radiation in narrow spectral bands. Reflectance is measured through a 28° field-of-view (FOV) aperture and incoming radiation is measured through a cosine-corrected sphere. Calibration is performed by pointing the 28° FOV aperture towards the sun using an opal glass. Using this calibration, spectral reflectances are derived. Specifications are given in table 2. Both field trials were measured a couple of times during the middle of the 2007 growing season. Trial 1 was measured on 20 June, 25 June, 2 July and 17 July. Trial 2 was measured on 14 June, 25 June, 2 July and 17 July. From the spectral measurements both WdVI and REP were calculated.

Statistical analysis

In this study focus is on the treatment effect of different levels of nitrogen fertilization. Main crop variable is the net tuber yield at harvest time. To test the N effect, a one-way analysis of variance (ANOVA) was performed on the yield

figures. The critical level shows whether there was a significant treatment effect. In addition, a pairwise Tukey test was applied to test which treatment effects were significant (at the 5% level).

Subsequently, both ANOVA and Tukey test were also applied to the spectral measurements obtained with the Cropscan and to the WDV and the REP. This should yield the best indicator for mapping the N effects and thus to discriminate growth differences as a result of differences in nitrogen status.

Next, a regression analysis was applied to study the relationship between spectral indicators and field measured tuber yield. The predictive power of the indices was assessed by estimating the root mean square of prediction ($RMSE_{pred}$) using the leave-one-out method.

As a final step we will investigate whether the results can be used to assess the optimal N level for both field trials individually.

RESULTS AND DISCUSSION

Potato yield figures

Figures 1 and 2 illustrate the final tuber yield as a function of the N fertilization level for trial 1 and 2, respectively. A second order polynomial function was fitted. Figure 1 shows for trial 1 that the yield increases with N level. Yield is low without N application. Based on these observations, highest yield is obtained with the highest N application of 260 kg/ha. Figure 2 shows less differences between the N levels for trial 2. The zero level (N0) is not as low as for trial 1. Moreover,

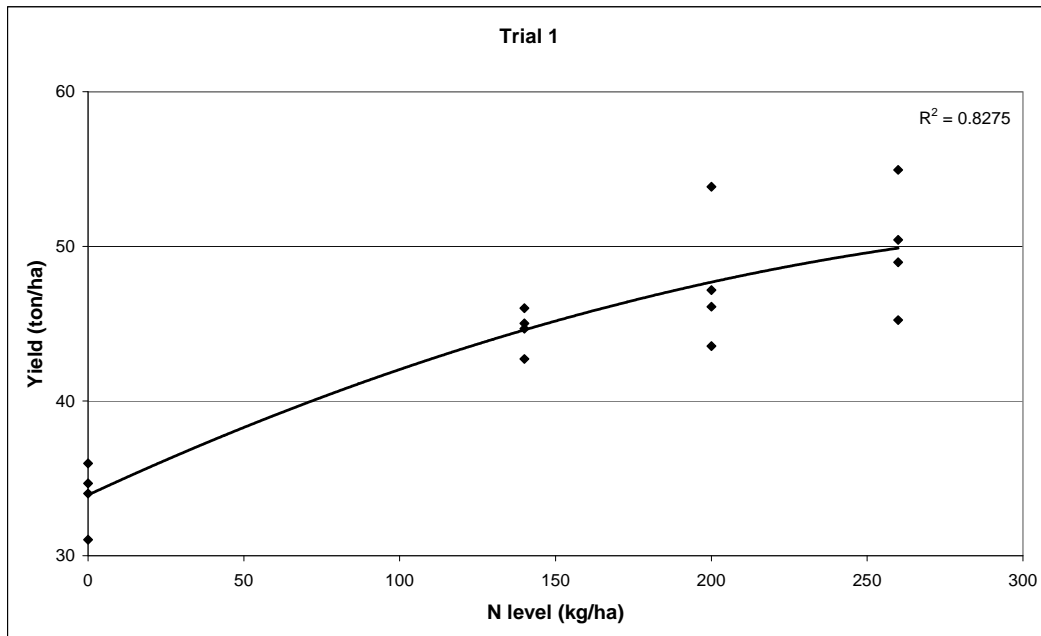


Figure 1. Tuber yield as a function of N fertilizer level for trial 1.

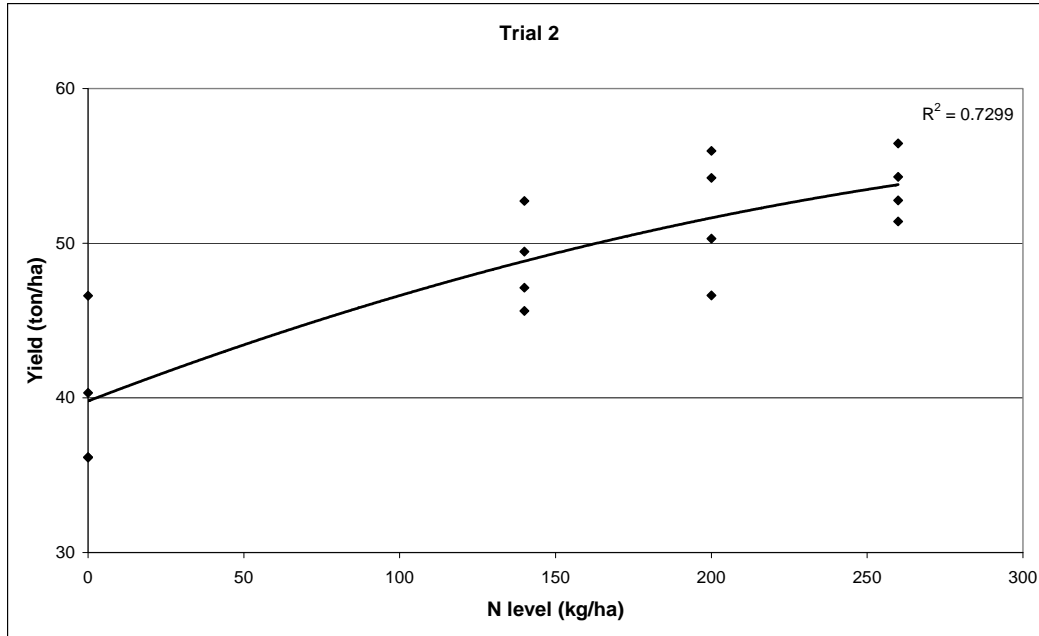


Figure 2. Tuber yield as a function of N fertilizer level for trial 2.

the N2 level (recommended level) seems to be optimal. Higher yields are obtained and less nitrogen fertilization is required for trial 2 as compared to trial 1. This may be caused by the more humous soil, keeping a higher moisture and mineralisation level during the season and thus giving better growing conditions.

Table 3 provides the results for the ANOVA. For both trials there is a significant N effect. Table 4 gives the results of the Tukey test, showing that there is only a significant pairwise difference between N0 and the other three N levels for both trials. N1, N2 and N3 are mutually not significantly different (at 5% significance level).

Table 3. ANOVA results for tuber yields in testing N fertilization of trial 1 and 2 (significance at the 5% level is indicated by grey blocks).

	Critical level
Trial 1	0.000
Trial 2	0.003

Table 4. Results of pairwise Tukey test for N levels of trial 1 and 2.

N level comparison	Trial 1	Trial 2
N0 - N1	0.003	0.039
N0 - N2	0.000	0.008
N0 - N3	0.000	0.003
N1 - N2	0.487	0.688
N1 - N3	0.117	0.319
N2 - N3	0.714	0.888

Spectral signatures

Figures 3 and 4 offer the average spectral signatures per N level for the measurements on 2 July 2007 as an example. Similar signatures were obtained for the other dates. From these the WDWI and REP were also calculated. The WDWI

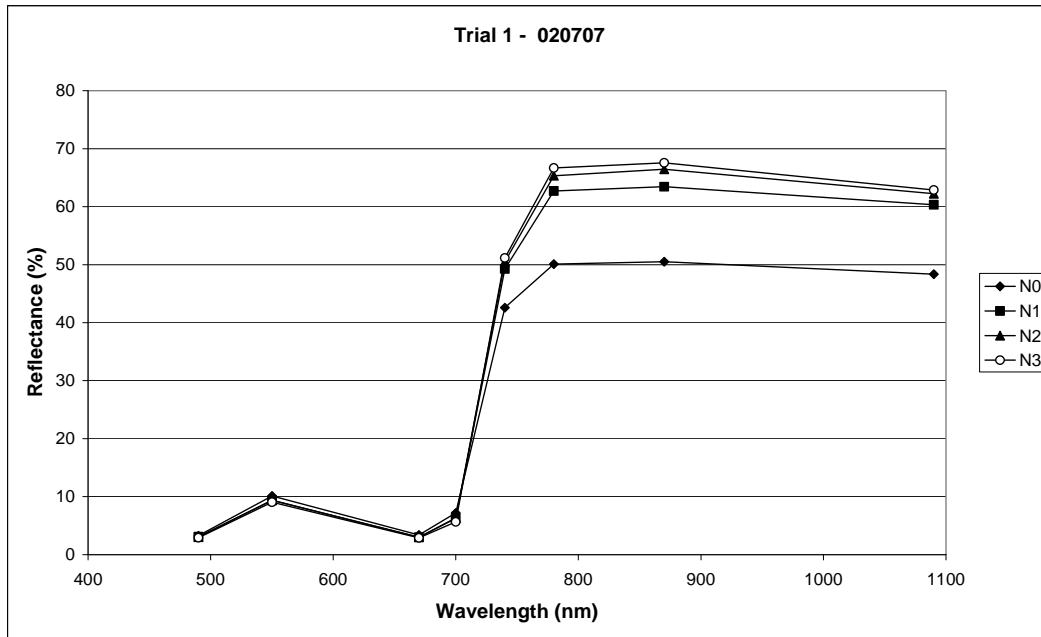


Figure 3. Example of the spectral signature of the different N fertilizer levels for trial 1 on 2 July 2007.

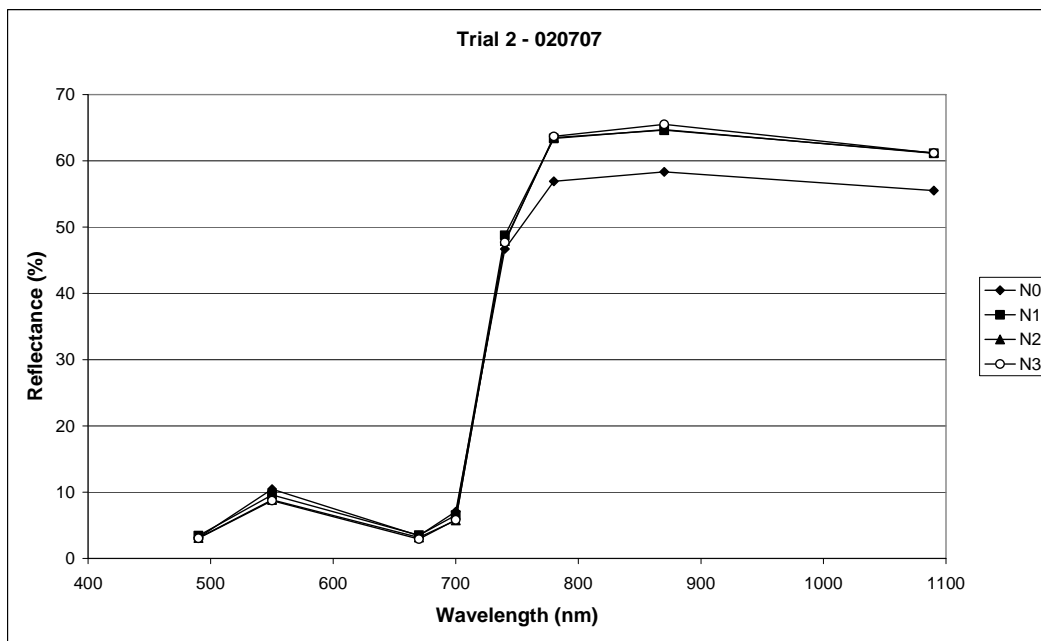


Figure 4. Example of the spectral signature of the different N fertilizer levels for trial 2 on 2 July 2007.

(and also the NIR reflectance) for both trials is clearly lower for the N0 level on all dates. However, the N0 level is higher for trial 2 than for trial 1. This was also shown before in terms of tuber yield.

Tables 5 and 6 provide the results for the ANOVA for trial 1 and 2, respectively, for all spectral bands, WDVl and REP. The N effect appears to be most significant for REP on 2 July and 17 July. On the measurement dates in June 2007, WDVl and NIR reflectances provide the most significant N effect. Tables 7 and 8 give the results of the Tukey test for WDVl and tables 9 and 10 those for the REP. Again there is a significant pairwise difference between N0 and the other three N levels for both trials. N1, N2 and N3 mostly are mutually not significantly different. In some cases there is a significant difference between N1 and N3. This is in particular the case for the REP.

Table 5. ANOVA results (F values) with respect to N test for spectral measurements of trial 1 (significance at the 5% level is indicated by grey blocks; $F_9^3(0.05) = 3.86$).

	20 June	25 June	2 July	17 July
490 nm	2.44	0.86	0.78	1.26
550 nm	1.92	0.45	9.68	13.84
670 nm	0.12	0.97	3.05	0.56
700 nm	1.14	0.64	17.49	12.74
740 nm	23.19	34.73	15.85	17.42
780 nm	34.85	54.31	29.97	30.96
870 nm	37.21	50.52	34.26	36.95
1090 nm	38.56	44.60	34.07	31.67
WDVI	35.05	69.34	35.31	29.40
REP	24.25	5.26	132.67	42.49

Table 6. ANOVA results (F values) with respect to N test for spectral measurements of trial 2.

	14 June	25 June	2 July	17 July
490 nm	11.91	2.68	3.61	1.57
550 nm	8.57	9.16	28.83	51.02
670 nm	4.59	1.42	6.10	6.62
700 nm	3.63	1.55	19.91	44.15
740 nm	49.34	7.04	0.99	5.53
780 nm	70.39	20.04	9.65	15.84
870 nm	63.25	17.79	8.81	16.83
1090 nm	62.31	10.89	7.81	18.44
WDVI	56.10	18.97	11.56	17.90
REP	33.29	12.68	42.85	56.82

Table 7. Results of pairwise Tukey test for N levels of WDVl of trial 1.

N level comparison	20 June	25 June	2 July	17 July
N0 - N1	0.000	0.000	0.000	0.000
N0 - N2	0.000	0.000	0.000	0.000
N0 - N3	0.000	0.000	0.000	0.000
N1 - N2	0.738	0.451	0.448	0.418
N1 - N3	0.145	0.054	0.185	0.588
N2 - N3	0.624	0.463	0.901	0.988

Table 8. Results of pairwise Tukey test for N levels of WDVI of trial 2.

N level comparison	14 June	25 June	2 July	17 July
N0 - N1	0.000	0.002	0.013	0.006
N0 - N2	0.000	0.000	0.006	0.001
N0 - N3	0.000	0.001	0.002	0.000
N1 - N2	0.945	0.590	0.962	0.669
N1 - N3	0.660	0.754	0.531	0.210
N2 - N3	0.371	0.991	0.796	0.756

Table 9. Results of pairwise Tukey test for N levels of REP of trial 1.

N level comparison	20 June	25 June	2 July	17 July
N0 - N1	0.001	0.276	0.000	0.000
N0 - N2	0.001	0.058	0.000	0.000
N0 - N3	0.001	0.020	0.000	0.000
N1 - N2	1.000	0.713	0.108	0.169
N1 - N3	0.984	0.344	0.006	0.053
N2 - N3	0.972	0.894	0.248	0.858

Table 10. Results of pairwise Tukey test for N levels of REP of trial 2.

N level comparison	14 June	25 June	2 July	17 July
N0 - N1	0.001	0.014	0.000	0.000
N0 - N2	0.000	0.005	0.000	0.000
N0 - N3	0.000	0.001	0.000	0.000
N1 - N2	0.265	0.895	0.172	0.777
N1 - N3	0.035	0.315	0.116	0.025
N2 - N3	0.541	0.677	0.993	0.103

Relationship spectral indices with final tuber yield

Since WDVI and REP both show the differences in nitrogen fertilization as shown in the previous section, in this section the relationship of these indicators with tuber yield is studied. This analysis is done for both trials individually. Since it is expected that results for both trials individually yield similar relationships, the analysis is also done for both trials combined. Results in terms of R^2 and $RMSE_{pred}$ are given in table 11 and 12, respectively. Significant R^2 values are obtained in all cases. For both trials separately R^2 is significant at 5% level if $R^2 > 0.29$. For both trials combined this R^2 is 0.11. Table 12 shows that the WDVI yields an error ($RMSE_{pred}$) between 2.70 and 4.52 ton/ha. This means a range of 6% - 10% of average tuber yield. The error in yield prediction by the REP is between 3.79 and 5.72 ton/ha, which matches a range of 8% - 12% of the average tuber yield. Results for 2 July are illustrated in figures 5 and 6 for WDVI and REP, respectively. Relationships for both trials individually are similar, thus both indicators are also significantly correlated with tuber yield when both trials are combined.

Optimal nitrogen fertilization level

Figures 7 and 8 illustrate the WDVI as a function of the N fertilization level for trial 1 and 2, respectively. Again a second order polynomial function is fitted. Figure 7 shows for trial 1 that the WDVI for the N0 level is lower than for the other levels. WDVI keeps on increasing with increasing N level and the optimal N level seems to be around 260 kg/ha. This is the same result as for tuber yield. Figure 8 shows that for trial 2 differences between fertilization levels are less. Again the zero level (N0) is not as low as for trial 1. The optimal N level now is around 150 - 200 kg/ha. Results are similar to those obtained with tuber yield.

Table 11. Regression results in terms of R^2 (= coefficient of determination).

	WDVI			REP		
	Trial 1	Trial 2	Trial 1+2	Trial 1	Trial 2	Trial 1+2
14/20 June	0.88	0.83	0.87	0.46	0.71	0.57
25 June	0.81	0.66	0.74	0.63	0.46	0.50
2 July	0.82	0.84	0.71	0.73	0.63	0.71
17 July	0.79	0.73	0.61	0.71	0.66	0.66

Table 12. Regression results in terms of $RMSE_{pred}$ (= root mean square error of prediction).

	WDVI			REP		
	Trial 1	Trial 2	Trial 1+2	Trial 1	Trial 2	Trial 1+2
14/20 June	2.74	2.83	2.70	5.72	3.79	4.87
25 June	3.27	4.08	3.65	4.57	5.24	5.14
2 July	3.22	2.87	3.89	3.82	4.38	3.88
17 July	3.39	3.68	4.52	4.04	4.10	4.27

CONCLUSIONS

This study clearly shows that spectral measurements in the visible and near-infrared part of the spectrum can discriminate growth differences in potatoes as a result of differences in nitrogen status. Particularly the WDVl and REP were

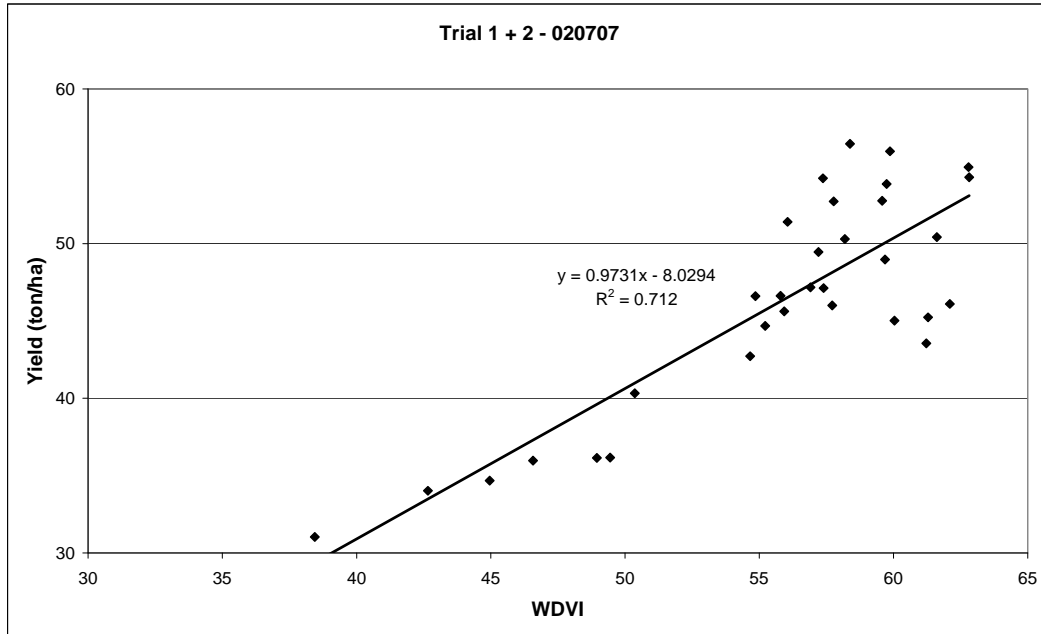


Figure 5. Example of the relationship between tuber yield and WDVl for trial 1 and 2 combined on 2 July 2007.

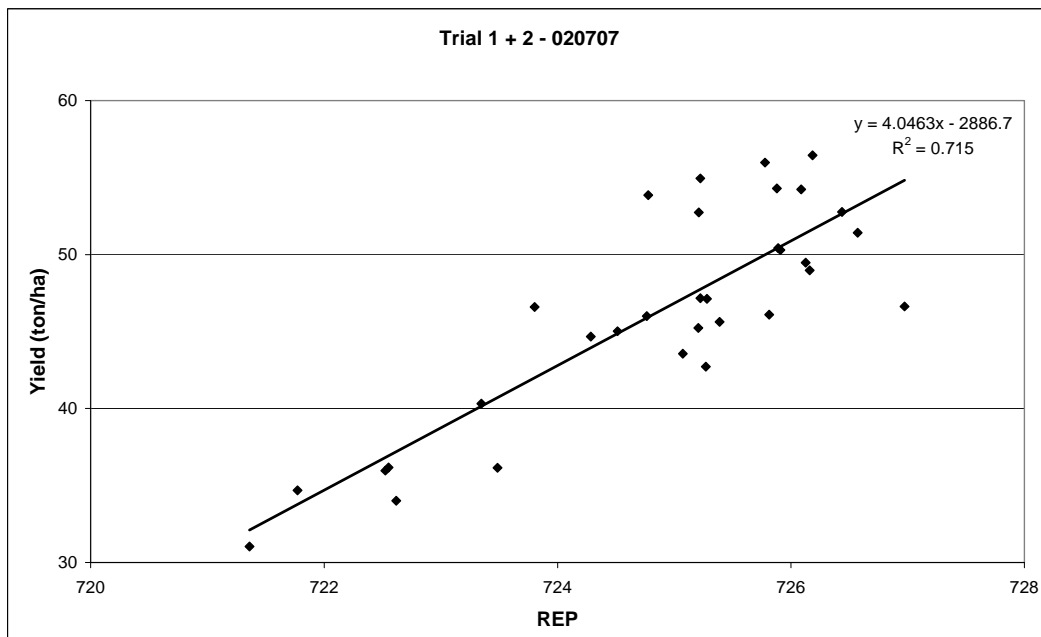


Figure 6. Example of the relationship between tuber yield and REP for trial 1 and 2 combined on 2 July 2007.

significantly correlated with the measured tuber yield at harvest time and can be used for determining the optimal N level for getting the highest yield. Further

research should focus on the question whether the resulting quality is also optimal.

At the moment biomass maps (see e.g. figure 9) are already produced from NIR digital imagery. Since atmospheric correction is a major complicating factor when

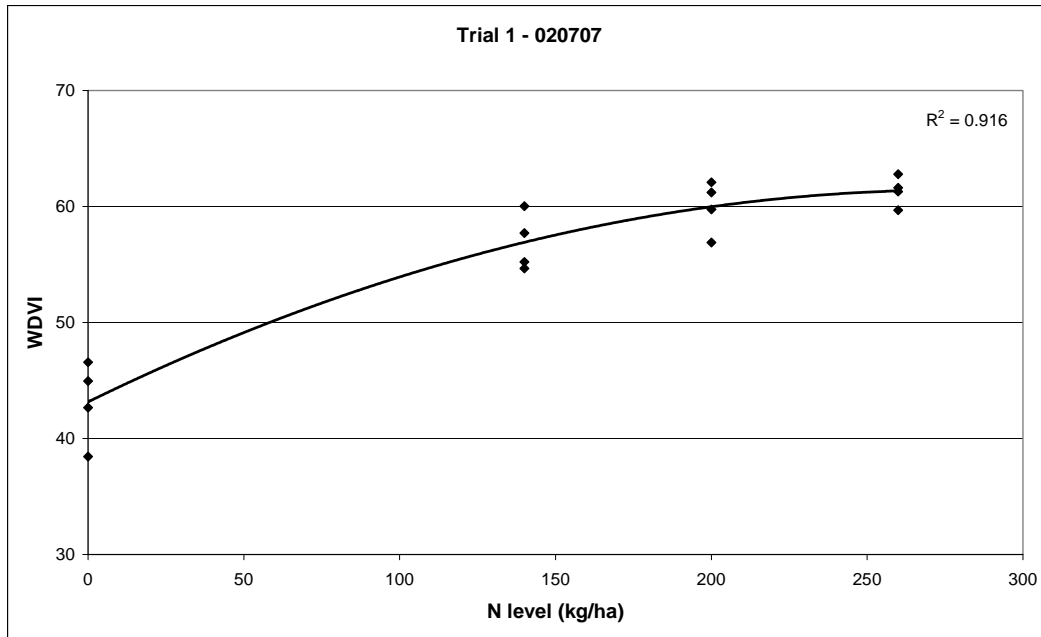


Figure 7. Example of the WDV I as a function of N fertilizer level for trial 1 on 2 July 2007.

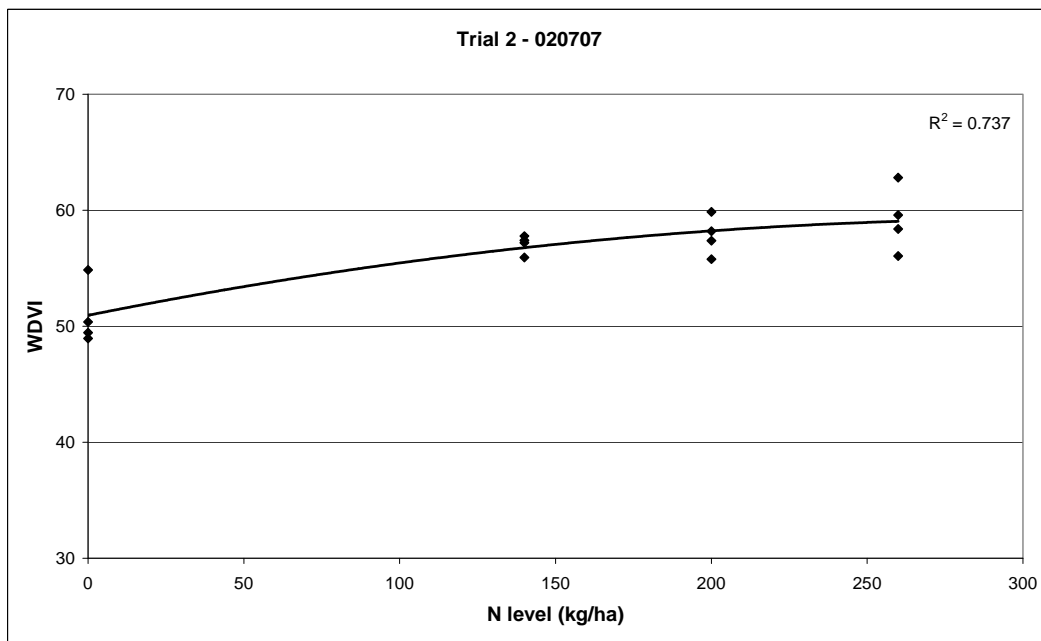


Figure 8. Example of the WDV I as a function of N fertilizer level for trial 2 on 2 July 2007.

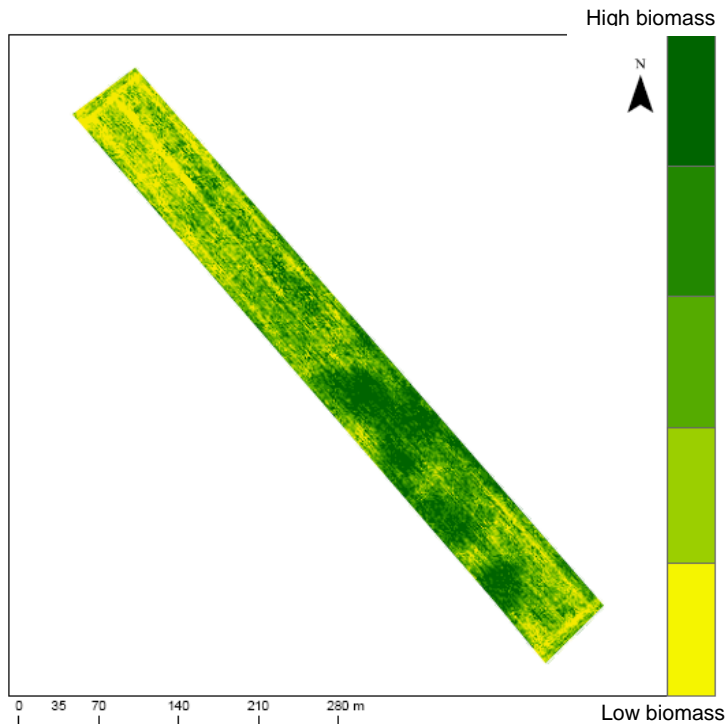


Figure 9. Example of a relative yield map derived from a digital image using a Canon infrared-enabled camera with internal infrared filter.

using airborne remote sensing data, currently only relative biomass maps are produced. However, these maps can be used for mapping relative differences within fields. For estimating REP, however, imaging spectroscopy data are required. Further research should provide the best methodology for determining optimal management practices. Remote sensing can be a valuable tool in this respect.

ACKNOWLEDGEMENTS

The field experiments were performed within the project “Perceel Centraal”, which is a collaboration between Agrifirm, Hilbrands Lab (HLB), Institute of Sugar Beet Research (IRS) and the Institute for Applied Plant Research (PPO) in the Netherlands.

REFERENCES

- Baret, F., Guyot, G., 1991. Potentials and limits of vegetation indices for LAI and APAR assessment. *Remote Sensing of Environment* 35(2-3), 161-173.
- Bouman, B.A.M., Van Kasteren, H.W.J., Uenk, D., 1992. Standard relations to estimate ground cover and LAI of agricultural crops from reflectance measurements. *ISPRS Journal of Photogrammetry & Remote Sensing* 4, 249-262.

- Broge, N.H., Leblanc, E., 2001. Comparing prediction power and stability of broadband and hyperspectral vegetation indices for estimation of green leaf area index and canopy chlorophyll density. *Remote Sensing of Environment* 76(2), 156-172.
- Clevers, J.G.P.W., 1988. Multispectral aerial photography as a new method in agricultural field trial analysis. *International Journal of Remote Sensing* 9(2), 319-332.
- Clevers, J.G.P.W., 1989. The application of a weighted infrared-red vegetation index for estimating Leaf Area Index by correcting for soil moisture. *Remote Sensing of Environment* 29(1), 25-37.
- Clevers, J.G.P.W., 1991. Application of the WdVI in estimating LAI at the generative stage of barley. *ISPRS Journal of Photogrammetry & Remote Sensing* 46(), 37-47.
- Clevers, J.G.P.W., 1999. The use of imaging spectrometry for agricultural applications. *ISPRS Journal of Photogrammetry and Remote Sensing* 54(5-6), 299-304.
- Clevers, J.G.P.W., Buker, C., van Leeuwen, H.J.C., Bouman, B.A.M., 1994. A framework for monitoring crop growth by combining directional and spectral remote sensing information. *Remote Sensing of Environment* 50(2), 161-170.
- Clevers, J.G.P.W., Jongschaap, R.E.E., 2001. Imaging spectrometry for agricultural applications. In F. D. Van der Meer et al, (Ed.), *Imaging Spectrometry: Basic Principles and Prospective Applications*, Kluwer Academic Publishers, Dordrecht, pp. 157-199.
- Clevers, J.G.P.W., Van Leeuwen, H.J.C., 1996. Combined use of optical and microwave remote sensing data for crop growth monitoring. *Remote Sensing of Environment* 56(1), 42-51.
- Clevers, J.G.P.W., Vonder, O.W., Jongschaap, R.E.E., Desprats, J.F., King, C., Prevot, L., Bruguier, N., 2002. Using SPOT data for calibrating a wheat growth model under Mediterranean conditions. *Agronomie* 22(6), 687-694.
- Daughtry, C.S.T., Walthall, C.L., Kim, M.S., Brown de Colstoun, E., McMurtrey III, J.E., 2000. Estimating corn leaf chlorophyll concentration from leaf and canopy reflectance. *Remote Sensing of Environment* 74(2), 229-239.
- Delecalle, R., Maas, S.J., Guerif, M., Baret, F., 1992. Remote sensing and crop production models: present trends. *ISPRS Journal of Photogrammetry & Remote Sensing* 47(2-3), 145-161.
- Guyot, G., Baret, F., 1988. Utilisation de la haute resolution spectrale pour suivre l'etat des couverts vegetaux. *Proceedings 4th International Colloquium 'Spectral Signatures of Objects in Remote Sensing'*, ESA, Paris, Aussois, France, pp. 279-286.
- Horler, D.N.H., Dockray, M., Barber, J., 1983. The red edge of plant leaf reflectance. *International Journal of Remote Sensing* 4(2), 273-288.
- Maas, S.J., 1988. Use of remotely-sensed information in agricultural crop growth models. *Ecological Modelling* 41(3-4), 247-268.
- Wessman, C.A., 1994. Estimating canopy biochemistry through imaging spectrometry. In J. Hill et al, (Ed.), *Imaging Spectrometry - A Tool for Environmental Observations*, Kluwer Academic, Dordrecht, pp. 57-69.